Modeling of Cr^{3+}-Doped Cs_2CdCl_4 Single Crystal

R. Kripal*

EPR Laboratory, Department of Physics, University of Allahabad, Allahabad-211002, India

Crystal field parameters of the Cr^{3+}-doped Cs_2CdCl_4 single crystal are determined by the superposition model. The zero-field splitting parameter D is then evaluated employing microscopic spin Hamiltonian theory. The theoretical zero-field splitting parameter for Cr^{3+} in Cs_2CdCl_4 single crystal at the axial symmetry site is in good agreement with the experimental value. The local distortion is considered to find the crystal field parameters.

topics: inorganic compounds, crystal fields, optical properties, electron paramagnetic resonance

1. Introduction

Electron paramagnetic resonance (EPR) is useful in obtaining information about the local site symmetry and zero-field splitting (ZFS) parameters of transition ions doped in different crystals [1, 2]. It also identifies the defects responsible for the charge compensation in the system. Cr^{3+} is one of the most investigated transition metal ions with $3d^3$ electronic configurations and $^4A_2$ ground state for the electron paramagnetic resonance [3].

Due to the combined effect of the crystal field and the spin–orbit coupling, the principal mechanism for the zero-field splitting of the ground state of $3d^3$ ions is the spin–orbit interaction from an admixture of higher multiplets [4]. The superposition model (SPM) has been useful in finding the crystal field parameters and spin Hamiltonian parameters for several $3d^n$ ions [5, 6].

Inorganic metal halide perovskites like Cs_2CdCl_4 are important due to their intriguing properties, such as tunable band gaps [7] and long carrier diffusion lengths [8]. These inorganic metal halide perovskites are investigated as promising materials for various applications, including solid-state lighting [9], photocatalysis [10], photovoltaics [11], and thermoelectric [12]. These materials, when doped with transition metal ions, are of particular interest due to their extensive applications in light-emitting display technologies, optoelectronics, lasers, solar cells, and biomedical imaging [13]. The optical and scintillation properties of undoped, Sb^{3+}-doped, and Tl^+-doped Cs_2CdCl_4 single crystals were investigated. The light yield of undoped Cs_2CdCl_4 is enhanced by doping with Sb^{3+} and Tl^+. The thermally stimulated luminescence characteristics are also achieved by doping with Sb^{3+} [14].

The EPR study of Cr^{3+} ion doped in various single crystals has been done due to the zero-field splitting of this ion being quite sensitive to small distortion in the lattice. EPR study of Cr^{3+} ion in Cs_2CdCl_4 crystal has been reported [15]. It is important to find the site of the paramagnetic impurity Cr^{3+}, whether substitutional or interstitial, when incorporated in Cs_2CdCl_4. EPR study [15] indicated that Cr^{3+} ion substitutes at the Cd^{2+} ion site with charge compensation and uncompensation. The EPR spectra of Cs_2CdCl_4 crystals doped with trivalent chromium suggest three distinct Cr^{3+} centers. Two of the centers have axial symmetry about the crystallographic c-axis while the third exhibits a rhombic one. The rhombic Cr^{3+} centers occupy four orientationally distinct sites in the Cs_2CdCl_4 crystals. Two structurally distinct types of Cs^+ ions surround a Cr^{3+} ion occupying a cadmium site. There are eight equivalent Cs^+ (1) ions and two equivalent Cs^+ (2) ions. A deficiency of one Cs^+ ion from either group will balance the charge discrepancy. If one of the Cs^+ (1) ions is missing, the symmetry at the Cr^{3+} ion is reduced. The zero-field splitting tensor for a Cr^{3+}–Cs^+ (1) center should be rhombic [15]. As any of the eight Cs^+ (1) ions could be lost, there are eight possible orientations for the Cr^{3+}–Cs^+ (1) center in the Cs_2CdCl_4 lattice. Four orientations are distinguishable by EPR [15]. These orientations become equivalent when the magnetic field is along the crystallographic a-, b-, or c-axes. If one of the two Cs^+ (2) ions is missing, the symmetry at the Cr^{3+} ion is only reduced to C_{4v}, and the center is axial. Only one magnetically distinguishable orientation for the Cr^{3+}–Cs^+ (2) center is obtained [15]. The one axial center results from an uncompensated Cr^{3+} ion and is designated as Cr^{3+}–(0) (Center I). The other axial centers can be attributed to Cr^{3+} ions which are associated with Cs^+ (2) deficiencies, Cr^{3+}–Cs^+ (2) (Center II) [15].

The EPR parameters, namely zero-field splitting D, the g factors $g_\parallel$ and $g_\perp$, and hyperfine structure constants $A_\parallel$ and $A_\perp$ of Ti^{2+} and V^{3+} ($3d^2$) ions in CdS crystals with trigonal symmetry have been determined by applying the high-order perturbation formulae based on the cluster approach [2]. The local lattice distortion of a Cr^{3+}–(0) center (Center I) in a Cs$_2$CdCl$_4$ crystal has been studied by fitting the calculated EPR parameters D, $g_\parallel$, and $g_\perp$ to the experimental values with semi-SCF d-orbit wave functions model and perturbation loop method in a tetragonal strong field scheme [16].

In the present investigation, the ZFS parameter D for the Cr^{3+} ion in Cs$_2$CdCl$_4$ (Center I, II) is evaluated using crystal field parameters from the superposition model and perturbation equation. The thus obtained ZFS parameter D matches well with the experimental value. The present method gives a better match of calculated D with the experimental value compared to earlier studies [2, 16]. In addition, crystal field (CF) energy values are also computed and compared with the experimental values in the present investigation.

2. Crystal structure

The Cs$_2$CdCl$_4$ crystal is tetragonal with $a = 5.26$ and $c = 16.88$ Å, $Z = 2$ [17]. The space group is $I4/mmm$, and the crystal is isostructural with K$_2$NiF$_4$ [18]. Atoms are in the following positions: 4Cs in (e), $z = 0.357$, 2Cd in (a), 4Cl I in (c), and 4Cl II in (e), with $z = 0.149$. The structure is presented in Fig. 1. The local site symmetry at the Cr^{3+} ion is tetragonal or axial.

The crystallographic axis system CAS (a, b, c) is taken as shown in Fig. 1. A common axis system ($a \parallel x$, $b \parallel y$, $c \parallel z$) is taken to simplify the calculations.

3. Theoretical aspect

The ZFS parameter of the Cr^{3+} ion is obtained using the microscopic spin Hamiltonian (MSH) theory [19]. Taking the ZFS and Zeeman terms, the effective spin Hamiltonian for Cr^{3+} ions at axial symmetry is given by [5]

$$\mathcal{H} = D \left[S_z^2 - \frac{1}{3} S(S+1) \right] + \mu_B g_\parallel \, B_z S_z$$

$$+ \mu_B g_\perp \left(B_x S_x + B_y S_y \right), \tag{1}$$

where $g_\parallel$ and $g_\perp$ are the spectroscopic splitting factors, μ_B is the Bohr magneton, S is the electronic spin, $\boldsymbol{B} = (B_x, B_y, B_z)$ is the external magnetic field, and D is the second rank axial ZFS parameter.

For a doped crystal, the crystal field is given as

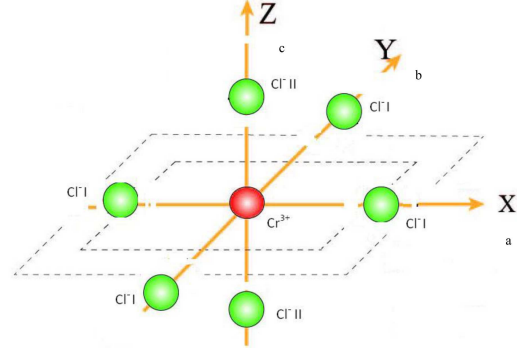$$\mathcal{H}_c = \sum B_{kq} C_q^{(k)}, \tag{2}$$

Fig. 1. Ligands around Cr^{3+} in Cs$_2$CdCl$_4$ with symmetry adopted axis system (SAAS).

where B_{kq} are the crystal field parameters in Wybourne notation and $C_q^{(k)}$ are the Wybourne spherical tensor operators.

In Cs$_2$CdCl$_4$ single crystal, the local symmetry around Cr^{3+} ions is axial. In axial symmetry, the ZFS parameter D is given by [5]

$$D = \frac{1}{2} \left[\varepsilon \left(\left| E' \left({}^4F \downarrow {}^4A_{2g} \downarrow {}^4B_1 \right) \right\rangle \right) \right.$$

$$\left. - \varepsilon \left(\left| E''({}^4F \downarrow {}^4A_{2g} \downarrow {}^4B_1) \right\rangle \right) \right], \tag{3}$$

where the free-ion ${}^4F$ ground term of $3d^3$ (Cr^{3+}) ions splits in octahedral symmetry into ${}^4A_{2g}$, ${}^4T_{2g}$, and ${}^4T_{1g}$ states, ${}^4A_{2g}$ being the ground state, and not split in the axial field, but its irreducible representation changed into ${}^4B_1$. Due to the combined action of the axial field and magnetic interactions, ${}^4B_1$ will split further, and this is expressed by group theory as $B_1 \otimes D^{(3/2)} \rightarrow B_1 \otimes (E' \oplus E'') \rightarrow E' \oplus E''$; the value of splitting is $2D$, where D is ZFS parameter of the ground state. Diagonalization of full Hamiltonian matrices yields the energy levels and eigen-vectors in terms of B_{kq}, B, C, and ξ, where B_{kq} are defined above; B and C are Racah parameters giving electron–electron repulsion, and ξ is the spin–orbit coupling parameter. In terms of average covalency parameter N, the Racah parameters [20–22] and the spin–orbit coupling parameter can be written, respectively, as

$$B = N^4 B_0, \quad C = N^4 C_0, \quad \text{and} \quad \xi = N^2 \xi_0, \tag{4}$$

where B_0 and C_0 are Racah parameters for free ion and ξ_0 is free ion spin orbit coupling parameter. For the Cr^{3+} ion, $B_0 = 918$ cm^{-1}, $C_0 = 3850$ cm^{-1}, and $\xi_0 = 276$ cm^{-1} are taken [21, 22].

Taking the values of Racah parameters ($B = 516$ cm^{-1}, $C = 3797$ cm^{-1}) found in the optical study of Cr^{3+}-doped crystal having halide (fluorine) ligands [23], the average covalency parameter $N = 0.9568$ is obtained employing

$$N = \frac{1}{2} \left(\sqrt{\frac{B}{B_0}} + \sqrt{\frac{C}{C_0}} \right). \tag{5}$$

TABLE I

Fractional position of Cr^{3+} ion along with spherical coordinates (R, θ, ϕ) of ligands in Cs_2CdCl_4 single crystal.

Position of Cr^{3+} (Fractional)	Ligands	x [Å]	y [Å]	z [Å]	Spherical coordinates of ligands		
					R [nm]	θ [°]	ϕ [°]
Site: Substitutional Cd1 $(0, 0, 0)$	Cl I(1)	0	0.5	0	0.2630	90	90
	Cl I(2)	0.5	0	0	0.2630	90	0
	Cl II(1)	0	0	0.149	0.2515	0	45
	Cl II(2)	0	0	−0.149	0.2515	180	45

4. Results and discussion

The SPM yields the crystal field parameters [24, 25] as

$$B_{kq} = \sum_j \overline{A_k}(R_j) K_{kq}(\theta_j, \varphi_j), \qquad (6)$$

where the coordination factor $K_{kq}(\theta_j, \varphi_j)$ is an explicit function of the angular position of the ligand. The intrinsic parameter $\overline{A_\kappa}(R_j)$ is given by

$$\overline{A_k}(R_j) = \overline{A_k}(R_0) \left(\frac{R_0}{R_j} \right)^{t_k}, \qquad (7)$$

where R_j is the distance of the d^n ion from the ligand, and, $\overline{A_k}(R_0)$ is the intrinsic parameter of the reference crystal, t_k gives the power law exponent, and R_0 is reference distance. Using the superposition model, the relation between the local structure parameters and crystal field parameters is written as [5]

$$B_{20} = -2\overline{A_2} \left(\frac{R_0}{R_{10}+\Delta R_1} \right)^{t_2} - 4\overline{A_2} \left(\frac{R_0}{R_{20}+\Delta R_2} \right)^{t_2}, \qquad (8)$$

$$B_{40} = 16\overline{A_4} \left(\frac{R_0}{R_{10}+\Delta R_1} \right)^{t_4} + 12\overline{A_4} \left(\frac{R_0}{R_{20}+\Delta R_2} \right)^{t_4}, \qquad (9)$$

$$B_{44} = 2\sqrt{70}\overline{A_4} \left(\frac{R_0}{R_{20}+\Delta R_2} \right)^{t_4}. \qquad (10)$$

Here, the reference distance R_0 is taken as 0.255 nm, which is slightly larger than the sum of ionic radii of the Cr^{3+} ion (0.0615 nm) and Cl^- ion (0.181 nm) [22]. Due to the incorporation of the impurity ion in the crystal, the local environment of the paramagnetic ion may be different from that of the host ion, and the bond lengths will change. The bond lengths may be expressed in terms of the distortion parameters ΔR_1 and ΔR_2, i.e., $R_1 = R_{10} + \Delta R_1$, $R_2 = R_{20} + \Delta R_2$. Note that $\overline{A_k}$ and t_k are already defined. For octahedral coordination, $\overline{A_4}$ is represented as [26]

$$\overline{A_4}(R_0) = \frac{3}{4}Dq. \qquad (11)$$

Using optical study [23], $Dq = 1494$ cm^{-1} and so the value of $\overline{A_4}(R_0) = 1120.5$ cm^{-1}. It should be noted that the ratio of $\overline{A_2}(R_0)$ and $\overline{A_4}(R_0)$

lies between 8 and 12 [21, 27, 28]. In the present investigation, $\frac{\overline{A_2}}{\overline{A_4}} = 10$ is taken, which gives $\overline{A_2} = 11205$ cm^{-1}. The crystal field parameters B_{kq} of Cr^{3+} ion in Cs_2CdCl_4 are calculated by taking the parameters $\overline{A_2}$ and $\overline{A_4}$, as well as the arrangement of chlorine atoms around the Cr^{3+} ion having matched experimental ZFS parameter. For the Cr^{3+} ion in Cs_2CdCl_4, the parameters $t_2 = 4$ and $t_4 = 6$ have been used. The position of the transition ion Cr^{3+} and the spherical coordinates of ligands when the Cr^{3+} ion substitutes the Cd^{2+} ion are shown in Table I. The ZFS parameter D of the Cr^{3+} ion in Cs_2CdCl_4 crystal is calculated from (3) [5]. The distortion parameters are taken as $\Delta R_1 = 0.1290$ nm and $\Delta R_2 = 0.1289$ nm with $R_{10} = 0.2572$ nm and $R_{20} = 0.2572$ nm for Center I. The distance R_{10} is the average of the Cr^{3+}–Cl^- I(1) and Cr^{3+}–Cl^- II(1) bond lengths, and R_{20} is the average of the Cr^{3+}–Cl^- I(2) and Cr^{3+}–Cl^- II(2) bond lengths. The distortion parameters for Center II are $\Delta R_1 = 0.0810$ nm, $\Delta R_2 = 0.0816$ nm with $R_{10} = 0.2572$ nm and $R_{20} = 0.2572$ nm. The calculated crystal field parameters and ZFS parameter, along with reference distance with distortion, are presented in Table II. The above parameters without distortion with the same reference distance also are given in Table II. The ZFS parameter calculated using crystal field parameters from the superposition model for both Centers I and II without distortion is larger than the experimental value [15]. The ZFS parameter calculated employing crystal field parameters from the superposition model for both Centers I and II with distortion is in good agreement with the experimental value [15], as can be seen in Table II. With the help of B_{kq} parameters and the CFA program [29–30], the optical spectra of the Cr^{3+}-doped Cs_2CdCl_4 crystal are calculated. The energy levels of the impurity ion are computed by diagonalizing the complete Hamiltonian, which consists of the Coulomb interaction (in terms of B and C parameters), Trees correction, the spin–orbit interaction, the crystal field Hamiltonian, the spin–spin interaction, and the spin–other-orbit interaction. The computed energy values are shown in Table III (input parameters are given below), along with the experimental values [15] for comparison.

TABLE II

Crystal field (CF) parameters and zero-field splitting (ZFS) parameter D of Cr^{3+}-doped Cs_2CdCl_4 single crystal with and without distortion.

	ΔR_1 [nm]	ΔR_2 [nm]	R_0 [nm]	Crystal field parameters [cm^{-1}]			Zero-field splitting parameter $|D|$ ($\times 10^{-4}$) [cm^{-1}]
				B_{20}	B_{40}	B_{44}	
I	0.1290	0.1289	0.255	-12779.8	2599.255	1554.731	228.1
	0.0000	0.0000	0.255	-64902.6	29758.97	17784.39	4855.0
							228.0*
II	0.0810	0.0816	0.255	-21611.8	5732.773	3405.186	595.4
	0.0000	0.0000	0.255	-64902.6	29758.97	17784.39	4855.0
							595.0*

*Experimental [15]

TABLE III

Calculated energy band positions of Cr^{3+}-doped Cs_2CdCl_4 single crystal together with the experimental values for comparison.

Transition from $^4A_2(F)$	Observed energy bands [cm^{-1}] (Ref [23])	Calculated energy bands [cm^{-1}] with distortion	
		I	II
$^4T_{2g}(F)$	14948	13855, 14009, 14178, 14820, 14832, 14941	13747, 13940, 14098, 14920, 15026, 16603
$^2E_g(G)$	15263	15014, 15359	16825, 16975
$^4T_{1g}(P)$	20406	18818, 18995, 19163, 19881, 19946, 20872	19697, 19967, 20033, 20183, 20485, 20760

It is concluded from Table III that there is a reasonable match with the experimental energy values [23].

Input parameters are as follows: numbers of free ion parameters = 5; number of d shell electrons = 3; number of fold for rotational site symmetry = 1; Racah parameters in A, B, and C, spin–orbit coupling constant, and Trees correction are 0, 516, 3797, 240, and 70 cm^{-1}, respectively; number of crystal field parameters = 3; B_{20}, B_{40}, B_{44} are taken from Table II; spin–spin interaction parameter, $M0 = 0.0000$; spin–spin interaction parameter, $M2 = 0.0000$; spin–other-orbit interaction parameter, $M00 = 0.0000$; spin–other-orbit interaction parameter, $M22 = 0.0000$; magnetic field, $B = 0.0$ Gs; angle between magnetic field $\boldsymbol{B}$ and z-axis = 0.00 degree.

It is observed from Table II that considering a small lattice distortion gives good agreement between theoretical and experimental results. This suggests that the distortion model employed here is quite reasonable. The parameters ΔR_1 and ΔR_2 are positive, which shows that the bond length of Cr–Cl is larger than Cd–Cl. When distortion in the crystal is neglected, a larger value of D is obtained. Taking a small distortion, the calculated ZFS parameter D is very close to the experimental value. This indicates that local distortion plays an important role in the contribution to the ZFS parameter and therefore must be taken into account in the calculation.

5. Conclusions

Cr^{3+} ions substitute at Cd^{2+} sites in Cs_2CdCl_4 crystal. The differences of charge and ionic radii between Cr^{3+} and Cd^{2+} ions provide local distortion around Cr^{3+} impurity. The theoretical investigation of the ZFS parameter has been done using the perturbation formula and crystal field parameters found in the superposition model. Taking local distortion, the ZFS parameter values of Cr^{3+} ion in Cs_2CdCl_4 crystal for both Centers I and II are in good agreement with the experimental values. It has also been found that there is a reasonable agreement between the computed and experimental optical energy values. Thus the theoretical result supports the conclusion of the experimental study.

Acknowledgments

References

[1] J.A. Weil, J.R. Bolton, J.E. Wertz, *Electron Paramagnetic Resonance: Elementary Theory and Practical Applications*, Wiley, New York 1994.

[2] Z. Wen-Chen, W. Shao-Yi, D. Hui-Ning, Z. Jian, *Spectrochim. Acta A* **58**, 537 (2002).

[3] Y.Y. Yeung, D.J. Newman, *Phys. Rev. B* **34**, 2258 (1986).

[4] C. Rudowicz, P. Gnutek, M. Açıkgöz, *Appl. Spectrosc. Rev.* **54**, 673 (2019).

[5] Q. Wei, *Acta Phys. Pol. A* **118**, 670 (2010).

[6] Y.Y. Yeung in: *Optical Properties of 3d-Ions in Crystals: Spectroscopy and Crystal Field Analysis*, Ch. 3, Eds. N.M. Avram, M.G. Brik, Springer, 2013, p. 95.

[7] L. Protesescu, S. Yakunin, M. I. Bodnarchuk, F. Krieg, R. Caputo, C.H. Hendon, R.X. Yang, A. Walsh, M.V. Kovalenko, *Nano Lett.* **15**, 3692 (2015).

[8] B. Li, Y. Zhang, L. Fu, T. Yu, S. Zhou, L. Zhang, L. Yin, *Nat. Commun.* **9**, 1 (2018).

[9] M. Jiang, Z. Hu, Z. Liu, Z. Wu, L.K. Ono, Y. Qi, *ACS Energy Lett.* **4**, 2731 (2019).

[10] T. Wang, D. Yue, X. Li, Y. Zhao, *Appl. Catal. B* **268**, 118399 (2020).

[11] Y. Wang, D.M. Ibrahim, L.K. Ono et al., *Science* **365**, 591 (2019).

[12] H. Xie, S. Hao, J. Bao, T.J. Slade, G.J. Snyder, C. Wolverton, M.G. Kanatzidis, *J. Am. Chem. Soc.* **142**, 9553 (2020).

[13] M.P. Lewis, N. Keerthana, N.D. Hebbar, K.S. Choudhari, S.D. Kulkarni, *Curr. Appl. Phys.* **32**, 71 (2021).

[14] T. Sakai, M. Koshimizu, Y. Fujimoto, D. Nakauchi, T. Yanagida, K. Asai, *Sens. Mater.* **30**, 1564 (2018).

[15] D. Kay, G.L. McPherson, *J. Phys. C Solid State Phys.* **14**, 3247 (1981).

[16] T.X. Zeng, J.J. Chen, T.H. Chen, Z.X. Liu, Y. Huang, *Rad. Eff. Defects Solids* **164**, 187 (2009).

[17] S. Siegel, E. Gebert, *Acta Cryst.* **17**, 790 (1964).

[18] D. Balz, *Naturwissenschaften* **40**, 241 (1953).

[19] C. Rudowicz, *Magn. Reson. Rev.* **13**, 1 (1987).

[20] W.L. Yu, M.G. Zhao, *J. Phys. C Solid State Phys.* **18**, L525 (1984).

[21] A. Abragam, B. Bleaney, *Electron Paramagnetic Resonance of Transition Ions*, Clarendon Press, Oxford 1970.

[22] C.K. Jorgensen, *Modern Aspects of Ligand Field Theory*, North-Holland, Amsterdam, 1971, p. 305.

[23] R. Nistora, L. Andreici, N.M. Avram, *Acta Phys. Pol. A* **116**, 538 (2009).

[24] W.L. Yu, M.G. Zhao, *Phys. Rev. B* **37**, 9254 (1988).

[25] D.J. Newman, B. Ng, *Rep. Prog. Phys.* **52**, 699 (1989).

[26] D.J. Newman, B. Ng, *Crystal Field Handbook*, Cambridge University Press, Cambridge, 2000.

[27] D.J. Newman, D.C. Pryce, W.A. Runciman, *Am. Miner.* **63**, 1278 (1978).

[28] T.H. Yeom, S.H. Choh, M.L. Du, *J. Phys. Condens. Matter* **5**, 2017 (1993).

[29] Y.Y. Yeung, C. Rudowicz, *J. Comput. Phys.* **109**, 150 (1993).

[30] Y.Y. Yeung, C. Rudowicz, *Comput. Chem.* **16**, 207 (1992).